

Christoph Böhne, Gerson Meschut, Max Biegler, Michael Rethmeier

Avoidance of liquid metal embrittlement during resistance spot welding by heat input dependent hold time adaption

Journal article | Accepted manuscript (Postprint)

This version is available at <https://doi.org/10.14279/depositonce-10514>



This is an Accepted Manuscript of an article published by Taylor & Francis in Science and Technology of Welding and Joining on 20 Jul 2020, available online:
<http://www.tandfonline.com/10.1080/13621718.2020.1795585>.

Böhne, C., Meschut, G., Biegler, M., & Rethmeier, M. (2020). Avoidance of liquid metal embrittlement during resistance spot welding by heat input dependent hold time adaption. *Science and Technology of Welding and Joining*, 25(7), 617–624. <https://doi.org/10.1080/13621718.2020.1795585>

Terms of Use

Copyright applies. A non-exclusive, non-transferable and limited right to use is granted. This document is intended solely for personal, non-commercial use.

WISSEN IM ZENTRUM
UNIVERSITÄTSBIBLIOTHEK

Technische
Universität
Berlin

Avoidance of liquid metal embrittlement during resistance spot welding by heat input dependent hold time adaption

Christoph Böhne*^a, Gerson Meschut^a, Max Biegler^b & Michael Rethmeier^{b,c,d}

^aLaboratory for Material and Joining Technology (LWF), Paderborn, Germany;

^bFraunhofer Institute for Production Systems and Design Technology (IPK), Berlin, Germany; ^cFederal Institute for Materials Research and Testing (BAM), Berlin,

Germany; ^dInstitute for Machine Tools and Factory Management (IWF), Technical University of Berlin, Berlin, Germany;

Corresponding author:

Christoph Böhne, Christoph.boehne@lwf.uni-paderborn.de, phone: +49 5251 60 4916

Christoph Böhne (M.Sc.) studied mechanical engineering at the University of Paderborn and graduated in 2017. Currently he is working as a research assistant in the work group thermal joining with focus on resistance welding processes.

Prof. Dr.-Ing. Gerson Meschut, graduated in 1998 at the University of Paderborn in Mechanical Engineering. After continuing research as chief-engineer, he joined the research and development department of Volkswagen AG in Wolfsburg in 2000. From 2005 to 2011 he was the technical managing director of Wilhelm Böllhoff GmbH & Co. KG in Bielefeld. Currently, he is the head of the Laboratory for Materials and Joining Technology (LWF) of the University of Paderborn.

Max Biegler (M.Sc.) finished his studies in mechanical engineering at Technical University of Munich in 2015. He is currently working as a research associate at Fraunhofer IPK with focus on numerical modelling of welding processes.

Univ.-Prof. Dr.-Ing. Michael Rethmeier graduated in 2003 at the Technical University Carolo Wilhelmina Braunschweig in Mechanical Engineering. Before joining the Technical University of Berlin (TUB) and the Federal Institute for Materials Research and Testing (BAM) in 2007, he worked at the Volkswagen AG. Currently, he is head of department 'Welding Technologies' (BAM), the field of 'Joining Technologies' at the Institute for Machine Tools and Factory Management (TUB) and the department of 'Joining and Coating Technology' (Fraunhofer IPK).

Avoidance of liquid metal embrittlement during resistance spot welding by heat input dependent hold time adaption

Liquid metal embrittlement (LME) cracking can occur during resistance spot welding (RSW) in zinc coated advanced high strength steels (AHSS) for automotive production. In this study, a methodological variation of hold time is performed to investigate the process-related crack influence factors. A combination of numerical and experimental investigations confirms, that the extent of heat dissipation and re-heating of the sheet surface can be influenced and thus the degree of crack formation can be controlled in a targeted manner by the parameterisation of the hold time. The temperature and stress history of crack-free and crack-afflicted spot welds are analysed and a conclusion on the borders defining the LME active region is derived.

Keywords: Liquid metal embrittlement; crack; advanced high strength steels; resistance spot welding; hold time; heat input; simulation

Introduction

The consistent implementation of lightweight construction concepts by car manufacturers enables an increase in driving safety with a simultaneous reduction in emissions [1]. In this context, modern advanced high-strength steels (AHSS) are particularly suitable for pursuing lightweight construction strategies, due to their superior combination of elongation and tensile strength [2]. The most commonly used method for joining these materials is resistance spot welding (RSW) [3]. Since these steel grades are usually coated with a zinc layer for corrosion protection, the RSW process can cause liquid metal embrittlement (LME) cracks [4]. Stress-assisted penetration of liquefied zinc and solid-state zinc diffusion along the grain boundaries of the steel leading to a subsequent reduction of its structural cohesion are proposed as the prevailing mechanisms for the formation of these cracks [5]. As LME cracks can impair the load-bearing capacity of spots welds if extremely large and deep cracks occur

[6–8], it is important to develop an understanding of the dominant process-related influencing factors and to develop methods for mitigation and prevention.

A number of studies associate a high heat input with increased crack formation [9–12]. Because in the RSW process the required process heat is generated by Joule heating, an intensified crack formation is observed when using either an excessive weld time [13] or a very high welding current close to [14] or slightly above the spatter limit [15]. The increased occurrence of cracks observed in several studies [16–18] when welding dissimilar combinations of AHSS-LME test candidates and conventional steels (higher thickness or multiple sheets) can also be explained in this context: The dissimilar stack-ups allow for a higher spatter-free maximum weld current i.e. more heat input compared to similar AHSS-AHSS combinations and the heat generation is concentrated in the AHSS joining partner, because of its higher resistivity. In the context of avoiding LME, limiting the heat input to the amount required to achieve the desired spot diameter and minimizing the welding process duration are important measures. Ashiri et al. [9] develop dedicated welding schedules, which they find to be able to prevent the formation of LME in zinc coated TWIP steels and also allow for a bigger spatter free maximum nugget diameter. Wintjes et al. [18] also investigate dedicated welding schedules (i.e. pre-pulses and multi-pulses) and achieve a reduction of the LME severity by up to 30%. Di Giovanni et al. [15] investigate the effect of linear decreasing weld current profiles for a high heat input welding scenario. They show that weld current ramping can mitigate tensile stresses after electrode release inside the indentation and that the investigated current profile is able to reduce the liquid zinc time for the weld shoulder region. Both observed effects contribute to a decrease in cracking intensity, measured via the crack index.

The crack behaviour of AHSS grades with strength in the range of 600 MPa and a mild steel is investigated by Sigler et al. [10]. They vary the welding current over different combinations of number of pulses, electrode force and hold time. In this way they investigate the influence of the hold time in several steps in the range between 2 cycles (~ 33 ms) and 60 cycles (~1000 ms). By using longer hold time durations they achieve crack-free welds, while they observe significant crack occurrence within the electrode impression for welds with short hold time durations. No detailed analysis of the background is reported.

Kim et al. [12] investigate the influence of hold time by varying its duration in three stages from 14 to 24 to 34 cycles (567 ms). They find that a variation of the hold time length leads to a slight change in the crack behaviour.

Choi et al. [6] investigate the effect of three different hold times (20, 300, 1000 ms) for three distinct weld times (200, 400, 800 ms). They evaluate crack depth and number in metallographic cross-sections. Both factors increase for a given hold time as the weld time increases. They observe a reduction of surface cracks within the electrode indentation for elongated hold times. Surface cracks in HAZ increase for longer weld times but no clear effect for the variation in hold time is observable for this crack type. Cracks at the interface between the welded sheets only appear for a combination of highly increased weld times (800 ms) and very short hold times (20 ms). No further analysis is performed. Choi et al. [19] focus on the effect of electrode force during welding. Predominantly surface cracks inside the HAZ are observed. The dominance of this crack type is explained by the electrode contact situation: Its curved geometry causes the coincidence of tensile stresses and local temperatures above the zinc melting point for a longer period (~400 ms) just outside the indentation (i.e. inside the HAZ). Because most of this period is within the heating phase, the cracks are believed to

initiate during the weld time rather than during cooling. Significant crack growth due to increased weld time is observed and attributed to a higher liquid zinc contact time.

Therefore, thermal factors are believed to be dominant: It is assumed that cracks initiate regardless of the electrode force (3, 4 and 5 kN) and that further crack growth is dependent on the duration of the exposure to liquid zinc.

Choi et al. [11] investigate the impact of hold times on the formation of cracks at the sheet interface near the spot weld notch. They observe cracks only for short hold times (< 100 ms), while spot welds generated with hold times > 200 ms are crack free. Their subsequent FE-Analysis shows larger stresses for welds created with longer hold times indicating opposite results. They resolve this by identifying the temperature at electrode lift-off as the most critical factor. A lower temperature limits the amount of freely available zinc and thus reduces the formation of LME cracks.

This publication takes up the systematic parameter variation in the hold time investigated in the literature. It shows the influence of the hold time duration on crack formation by experiments on stack-ups consisting of a variable number of sheets (i.e. changed stack-up overall thickness) and analyses the underlying effects. Statements on the time of crack formation are derived and finally, practical guidance is given for mitigation of LME.

Materials and methods

Materials

Similar to [20] and [21], this study is part of a framework project, which includes a variety of AHSS materials of different strength classes to evaluate for LME susceptibility. These steels were anonymously secured and characterized by WorldAutoSteel, the global automotive steel producer consortium with 22 member

companies. An electrogalvanized (EG) dual phase (DP) steel of the strength class 1200 MPa (hereinafter called DP1200 HD; corresponds to VDA 239-100: CR850Y1180T-DH) is used as the investigated AHSS-material for the experiments described in this article. It has a yield strength of 1050 MPa, an ultimate tensile strength of 1220 MPa, and a sheet thickness of 1.58 mm. The DP1200 HD is combined with a hot-dip galvanized (HDG) 2.00 mm thick mild steel (hereinafter called mild steel) with a yield strength of 170 MPa, and an ultimate tensile strength of 310 MPa. Based on these materials, a two-sheet and a four-sheet stack-up were formed consisting of the DP1200 HD as top sheet and using the mild steel for all additional layers (Table 1).

Welding equipment and experimental design

The RSW was performed on a servo-electric pedestal x-type welding gun, using 1000 Hz medium frequency direct current (MF-DC). An external weld process recorder was used to record the welding processes. The electrodes were water cooled by a rate of 4 l/min. Electrode caps of the types A0-16-20-100 (hereinafter called A0-100), as specified in ISO 5821 were used [22].

This cap type has been chosen based on the results presented in [21] as, it was shown to allow for crack free RSWs even under adverse welding conditions (i.e. elongated weld times and high heat input), by reducing the degree of plastic deformation at the indentation area. This makes it possible to evaluate the influence of temperature on LME formation widely decoupled from the otherwise excessive plastic deformation occurring during elongated weld times. The experimental design is shown in Table 1 and is based around the welding conditions identified to typically cause intense LME formation (e.g. weld times of 1520 ms).

Table 1: Overview of the experimental setup

Electrode geometry	A0-100		
Electrode force	4.5 kN		
Weld current	9.3 kA		
Weld time	1520 ms		
squeeze time	200 ms		
Stack-ups	DP1200 HD mild steel	DP1200 HD mild steel mild steel mild steel	
Hold times	10 ms	200 ms	800 ms

RSWs generated by use of two different stack-ups, each welded with three different hold times are compared.

Throughout all trials, an electrode force of 4.5 kN, a weld time of 1520 ms and a squeeze time of 200 ms were applied. The maximum spatter free weld current of 9.5 kA was determined based on common industry standards [23] for the two-sheet stack-up. To ensure spatter free welds the weld current was set to be 200 A below the maximum spatter free weld current. The identical weld current was adopted to the four-sheet stack-up. For the identical parametrisation during current flow, the four-layer stack-up is expected to generate more Joule heating, based on its higher total resistivity, caused by the additional steel sheets. All welds made by use of the same stack-up can be compared based on an identical heat input, since these welding processes only differ in hold time duration. The investigations were performed on $45 \times 45 \text{ mm}^2$ specimen and five repetitions were used per factor.

Analysis and measuring methods

For the verification of cracks, the zinc coating was removed around each spot weld after welding by staining with 20 % hydrochloric acid. A visual inspection followed by a photographic documentation was subsequently performed. The specimens were cross sectioned through the middle region of the observed cracks based on the surface crack

appearance. If no cracks were observed in the surface view, the direction was chosen to be identical to the samples that showed cracks.

For a closer analysis of the stress development and transient temperatures during the welding processes, a finite element model, established in [20], was used. According to ISO/TS 18166 [24] the model was validated against experimental cross-sections and transient temperature measurement. In the prior work, a DP1000 material data set was validated and the same data set is utilized here with scaled up $R_{p0.2}$ and R_m values to account for the higher strength class of the DP1200 HD. The model has already been used successfully to predict crack locations during an LME enforcement test [20] and to explain an electrode geometry variation for LME crack prevention [21]. Comparable to the experiments presented in this study, the simulations were conducted for the A0-100 electrode geometry and three different hold times. The models comprised 11976 linear hexahedral elements for the two-sheet setup and 23952 elements for the four sheet setup. With local refinement in the weld zone and edge lengths of up to 0.2 mm, calculation times for the nonlinear, transient electro-thermomechanical simulations were 44 min and 108 min for the 2- and 4-sheet welds respectively. To account for the different materials and contact conditions, reference measurements were conducted for electrical and thermal contact conductivity. The predicted longitudinal-stresses and transient temperature developments at the most frequently observed experimental crack location 2.6 mm from the center of the electrode indentation were extracted.

Results and discussion

Systematic screening of hold time variation for differing stack-ups

Figure 1 shows the results of welds made by systematic studies of two stack-ups and three different hold times.

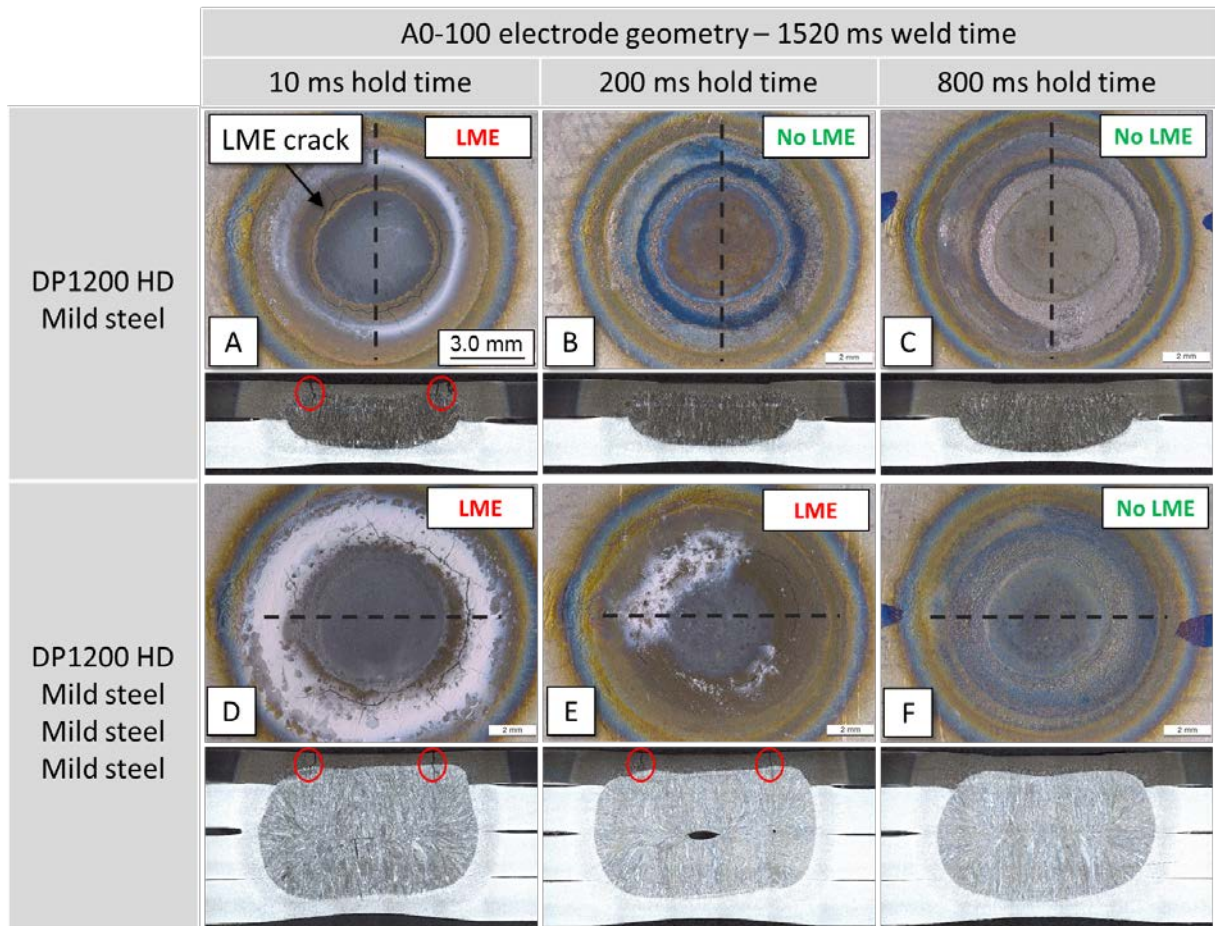


Figure 1: Weld process results from the three investigated hold times (left to right) and stack-ups (top and bottom) via surface view and cross-section.

The surface top views and corresponding cross-sections (A) – (C) show the results obtained for the two-sheet stack-up. (B) is showing a similar state as was investigated in [21]: Despite of the extremely elongated weld time, in case of a two sheet stack-up, a hold time of 200 ms results in crack free RSWs. For this stack-up a further increase of the hold time duration (C) is not necessary but also results in crack free weld joints. A significant reduction of the hold time to 10 ms (A), however, causes a reproducible formation of cracks.

The results of the investigations for the four-sheet stack-up are shown in (D) – (F). Unlike before, the use of a 200 ms long hold time (E) results in significant crack formation. A further shortening of the hold time to 10 ms (D) causes intensification of

the cracking, while an extension to 800 ms (F) can successfully prevent the formation of cracks for this four-sheet stack-up.

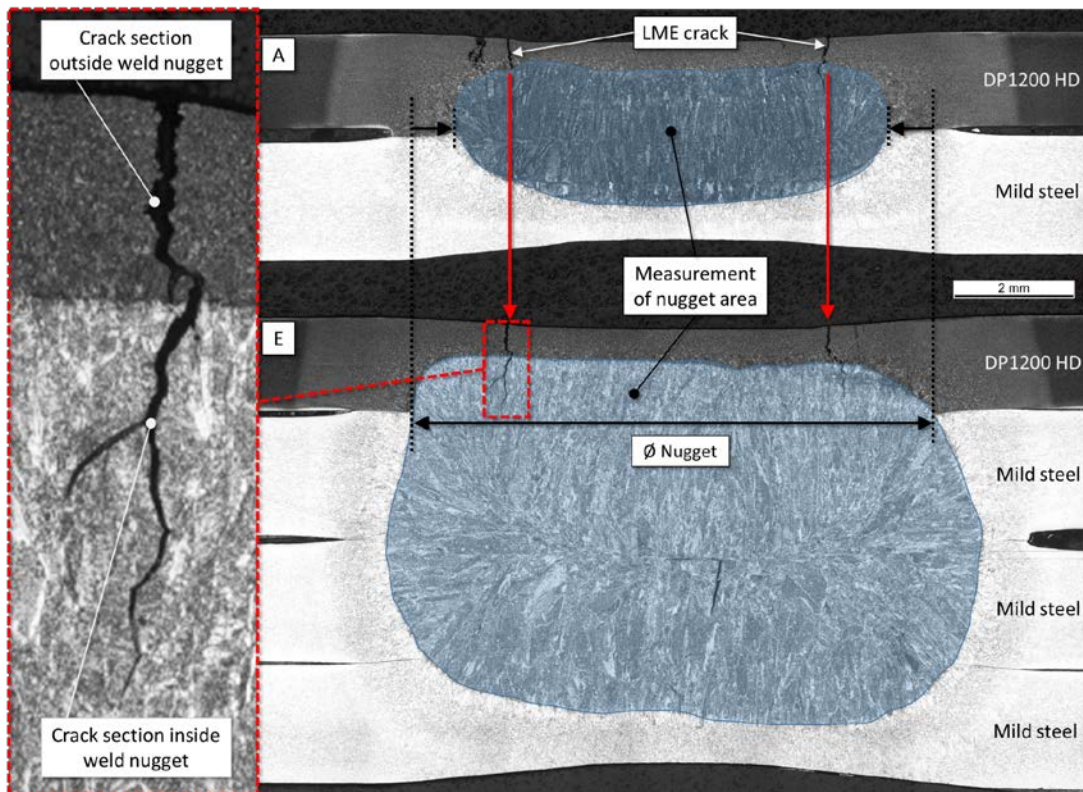


Figure 2: Cross-sectional comparison of weld nugget and crack formation for weld processes (A) and (E).

The cross-sections shown in Figure 2 compare spot welds created with the processes (A) and (E) and illustrate the diverging nugget dimensions for the two stack-ups. The added sheets cause an increase in dynamic resistance (Figure 3) for the four sheet stack-up, leading to an increased heat input by 45 % and a 20 % increased nugget diameter at the DP1200 HD to mild steel interface. The molten zone is enlarged from 15.7 mm² (two-layer stack-up) to 50.5 mm² (four-layer stack-up) in cross-section.

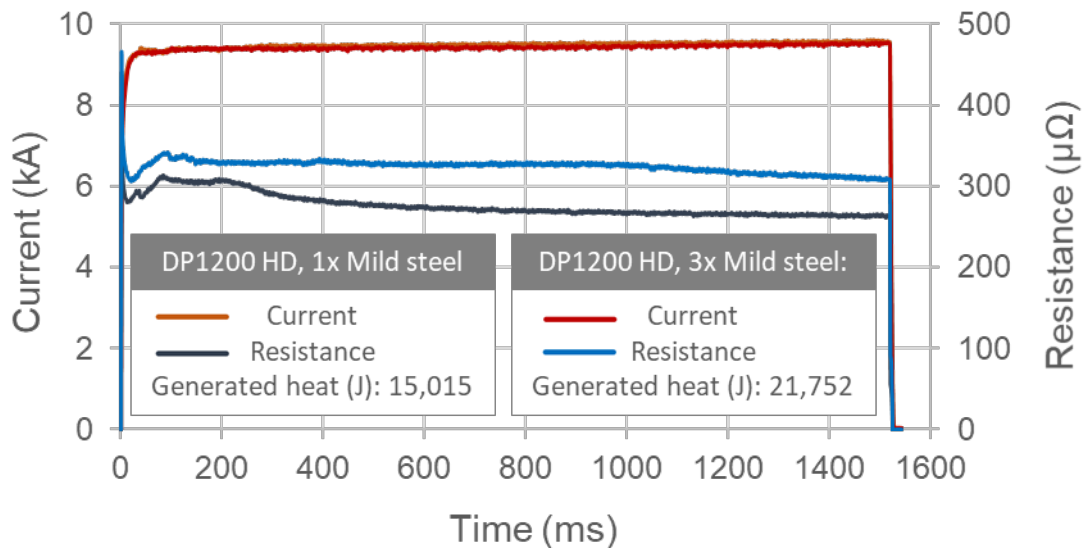


Figure 3: Weld process recording and calculated generated heat input.

The observed crack position on the circumference is similar in all cases. Cracks close to the center of the spot welds have not been observed. Figure 2 shows that for both investigated stack-ups, the cracks extend into the weld nugget. In [15] it is assumed that such cracks must have grown after nugget solidification. While this most certainly applies to the crack sections located within the nugget (see Figure 2) – as crack formation here can only occur during or after solidification of the nugget – further evidence is needed to prove that this applies to the crack sections located outside the nugget. The results presented in Figure 1 provide this evidence: The beginning of the crack formation is shown to take place after the end of the weld time for both investigated stack-ups, as the variation of the hold time duration is able to allow or entirely prevent the crack formation. In the following section, the finite element simulation will be used to analyse the temperature and stress history of the investigated spot welds to explain the observed behaviour.

Finite element simulation

The local process temperatures and x-stresses were calculated by use of the FE-simulation for a comparison between the two stack-ups, while considering the three

hold times. The locations correlate to the experimentally cracked spot weld regions highlighted in Figure 2. Figure 4 and Figure 5 show the corresponding plots for temperature and longitudinal stress on the sample surface at the crack afflicted region.

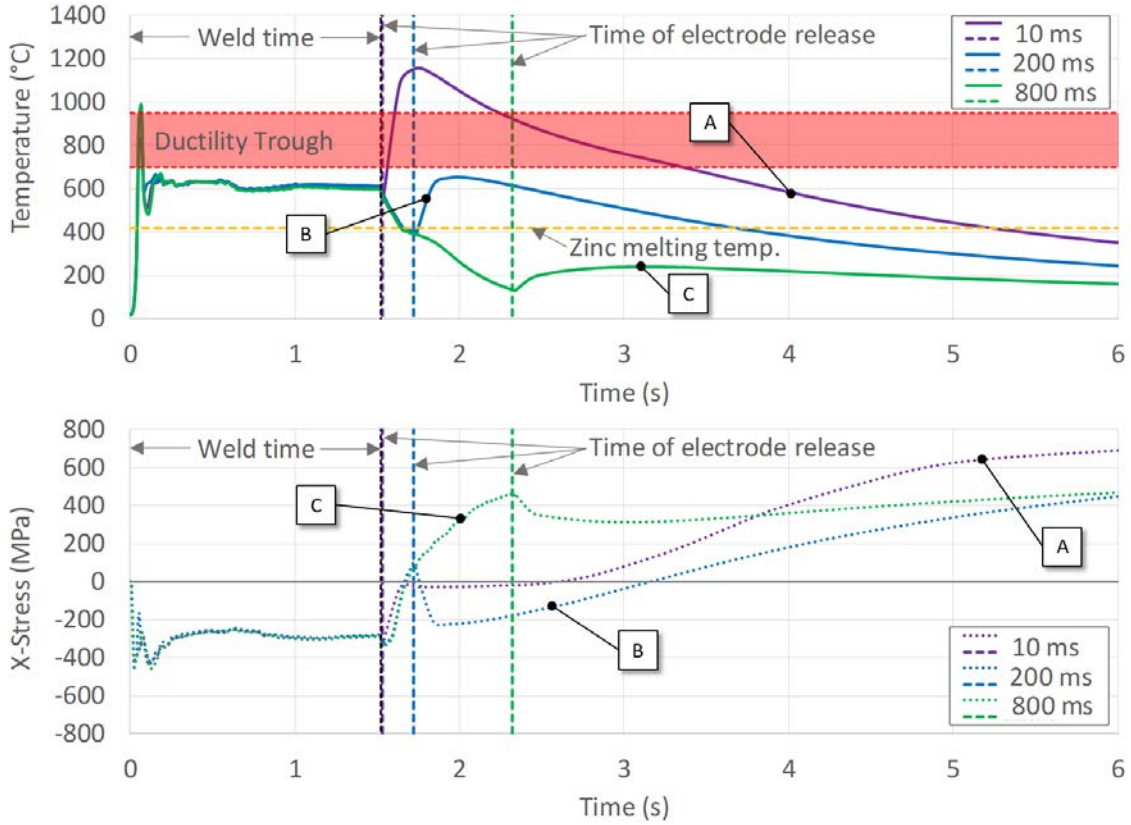


Figure 4: Temperature and x-stress plots for the crack location inside the electrode indent area of the two-sheet stack-up

All temperature plots show a re-heating at the end of the respective hold time, after electrode release. As a result of the higher heat generation within the four-sheet stack-up (Figure 5) the re-heating is more intense. Additionally, the cooling to temperatures below zinc melting temperature takes a longer period compared to the two-sheet stack-up. For both stack-ups, the level of the re-increase is significantly lowered for an increase in hold time duration.

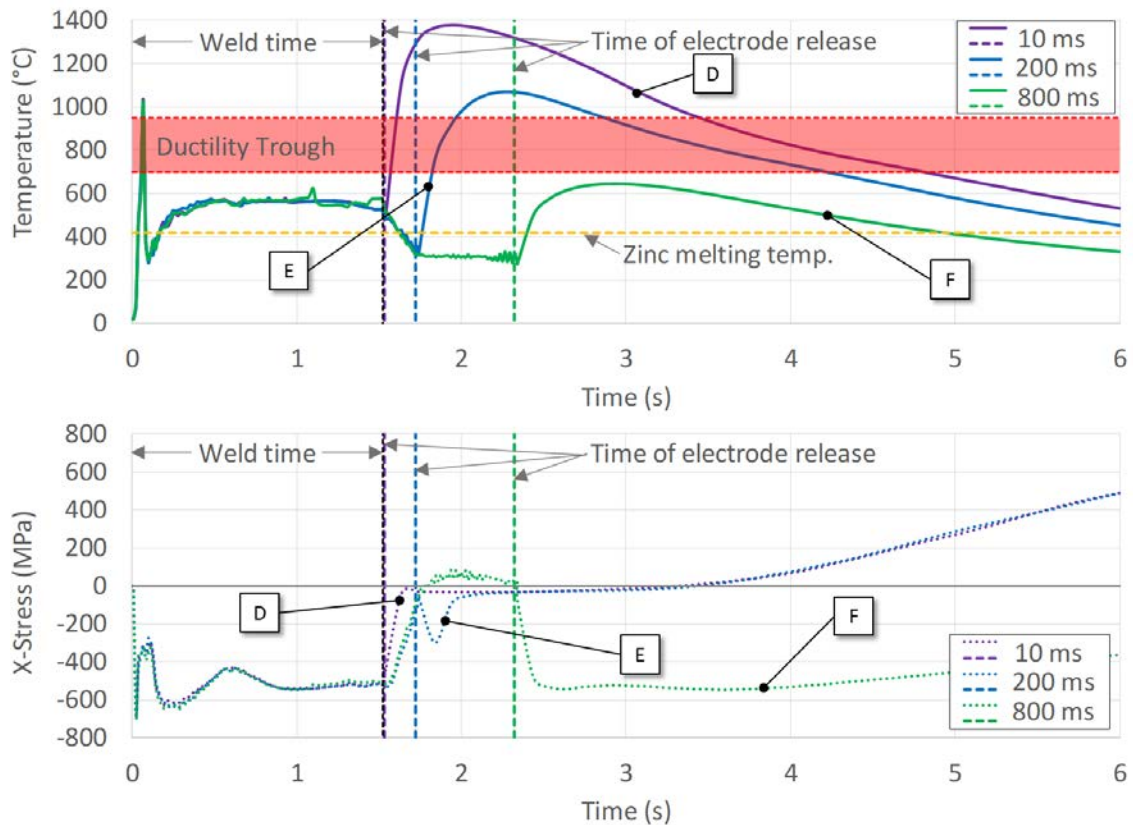


Figure 5: Temperature and x-stress plots for the crack location inside the electrode indent area of the four-sheet stack-up

For the weld scenarios (A) and (D) utilizing a 10 ms hold time, an intense reheating of the considered region to temperatures well above 1000°C can be observed. A simultaneous formation of tensile stresses is indicated by the x-stress plots. For the weld scenario (E) with 200 ms hold time, a minor but clear coincidence of temperatures above 700°C and the formation of tensile stresses can be observed, while for the two-sheet stack-up (B) the temperature during reheating stays below 700°C. The plots for the weld scenarios (C) and (F) show the lowest temperatures and x-stresses for both stack-ups, staying below 700°C during the whole welding process. In [7,11] the LME active region is characterised by an exceeding of the zinc melting temperature at 419°C (see Figure 4 and Figure 5) and experimental observations are based on the hypothesis that from this temperature on, a sufficient supply of liquid zinc creates the potential for the formation of LME cracks. Results generated in this study cannot entirely be explained with this definition of the LME active region:

The weld scenario (B) remains above the zinc melting temperature, and thus within the LME active region, for a significant period (~above 0.5 sec), while simultaneously experiencing increasing amounts of tensile stress. This definition of the LME active region cannot explain, why crack free welds are achieved for the welding scenario (B). In contrast, the temperature and x-stress plots correspond with the experimental results, when the LME active region is instead characterised by the so called “ductility trough” (see marker in Figure 4 and Figure 5). In [25] Béal determines this LME active region for TWIP steels to lie within a temperature range of 700°C to 950°C via hot tensile tests. This region could be linked to approaching the temperature of 782°C at which the dissolution of the protective intermetallic Fe-Zn compounds takes place and as a consequence high liquid zinc reactivity is predicted [26].

The upper limit of the ductility trough is defined similarly in many studies, as it is assumed to result from the evaporation of the zinc during the comparatively slow hot tensile test [5]. For the more dynamic RSW, however, the results show that a short but significant exceedance of the zinc evaporation temperature - see temperature plots for (A), (D) and (E) - does not lead to the evaporation of sufficient amounts of zinc, so that LME cracks can still be observed experimentally. As significantly extended welding processes (~1500 ms) have already been considered here, the relevance of the ductility trough upper limit for the RSW process can therefore be neglected. The lower limit of the ductility trough, serving as a marker for the LME active area, on the other hand, appears to have a high relevance: In this study the weld scenarios (A), (E) and (D) recreate an exposure to temperatures within the ductility trough and crack afflicted welds are experimentally observed. In parallel, for weld scenarios staying below this boundary (B), (C) and (F) experimentally crack free welds are achieved.

Conclusions

This study investigated a method for the controlling of LME during a low strain but high energy RSW-scenario of zinc coated AHSS grades and analysed the occurring effects by use of an FE-simulation. The combination of elongated weld time, high weld current and thick stack-ups cause a high accumulation of thermal energy within the joining zone, stressing the importance of the cooling capacity for a sufficient energy dissipation during hold time. The following conclusions can be derived from this study:

1. For the considered boundary conditions (i.e. A0-100 electrode caps and high heat input welding process), LME crack formation initiated entirely after the weld current switch-off (i.e. within or after the hold time).
2. The formation of LME cracks was caused or inhibited exclusively by selection of a specific hold time duration.
3. The hold time duration leading to cracked or crack free spot welds was dependent on the heat input (stack-up configuration). Higher heat-input welding scenarios require extended hold times.
4. LME cracks were only experimentally observed, if exposure to temperatures within the ductility trough coincided with the presence of tensile stresses, indicating a sufficient zinc availability only for regions heated significantly above the zinc melting temperature.
5. LME free spot welds for an extreme welding scenario (four-sheet stack-up with excessive energy input) were created by considering electrode geometry and hold time duration.

Acknowledgments

This work was supported by the WorldAutoSteel consortium, and was performed as part of a transnational study to further understand the basis for LME, and parameterization that achieves prevention or mitigation in BIW stack-ups involving AHSS.

Disclosure statements

No potential conflict of interest was reported by the authors.

References

- [1] Meschut G, Matzke M, Hoerhold R, et al. Hybrid Technologies for Joining Ultra-high-strength Boron Steels with Aluminum Alloys for Lightweight Car Body Structures. *Procedia CIRP*. 2014;23:19–23.
- [2] Schmitt J-H, Jung T. New developments of advanced high-strength steels for automotive applications. *Comptes Rendus Physique*. 2018;19:641–656.
- [3] Manladan SM, Abdullahi I, Hamza MF. A Review on the application of resistance spot welding of automotive sheets. *Journal of Engineering and Technology*. 2015;10:20–37.
- [4] Ling Z, Wang M, Kong L. Liquid Metal Embrittlement of Galvanized Steels During Industrial Processing: A Review. *Transactions on Intelligent Welding Manufacturing*. 2018:25–42.
- [5] Bhattacharya D. Liquid metal embrittlement during resistance spot welding of Zn-coated high-strength steels. *Materials Science and Technology*. 2018;34:1809–1829.
- [6] Choi D-Y, Uhm S, Enloe C, et al. Liquid Metal Embrittlement of Resistance Spot Welded 1180TRIP Steel - Effects of Crack Geometry on Weld Mechanical Performance. In: *Contributed Papers from MS&T17. Proceedings*; 08.10.2017 - 10.10.2017; 08.10.2017 - 10.10.2017; p. 454–462.
- [7] DiGiovanni C, Han X, Powell A, et al. Experimental and Numerical Analysis of Liquid Metal Embrittlement Crack Location. *J. of Materi Eng and Perform*. 2019;28:2045–2052.

- [8] DiGiovanni C, Biro E, Zhou NY. Impact of liquid metal embrittlement cracks on resistance spot weld static strength. *Science and Technology of Welding and Joining*. 2019;24:218–224.
- [9] Ashiri R, shamanian M, Salimijazi HR, et al. Liquid metal embrittlement-free welds of Zn-coated twinning induced plasticity steels. *Scripta Materialia*. 2016;114:41–47.
- [10] Sigler DR, Schroth JG, Yang W, et al. Observations of Liquid Metal-Assisted Cracking in Resistance Spot Welds of Zinc-Coated Advanced High-Strength Steels. In: *Sheet metal welding conference XIII. Proceedings*; May 14-16; Livonia, Michigan USA; 2008.
- [11] Choi D-Y, Sharma A, Jung JP. parametric study for liquid metal embrittlement in resistance spot welds of galvanized trip steel. In: *Sheet metal welding conference XVIII. Proceedings*; October 17-18; Livonia, Michigan USA; 2018.
- [12] Kim YG, Kim IJ, Kim JS, et al. Evaluation of Surface Crack in Resistance Spot Welds of Zn-Coated Steel. *Materials Transactions*. 2014;55:171–175.
- [13] Sierlinger R, Gruber M. A Cracking Good Story about Liquid Metal Embrittlement during Spot Welding of Advanced High Strength Steels. In: *Steels in Cars and Trucks 2017. Proceedings*; June 18-22; Noordwijkerhout / Amsterdam; 2017.
- [14] Frei J, Rethmeier M. Susceptibility of electrolytically galvanized dual-phase steel sheets to liquid metal embrittlement during resistance spot welding. *Weld World*. 2018;62:1031–1037.
- [15] DiGiovanni C, Bag S, Mehling C, et al. Reduction in liquid metal embrittlement

cracking using weld current ramping. *Weld World*. 2019;63:1583–1591.

[16] Benlatreche Y, Dupuy T, Mescolini D, et al. Design rules to minimize LME (Liquid Metal Embrittlement). Presented at: *Joining in Car Body Engineering 2019* - Bad Nauheim; April 9-11, 2019.

[17] C. Fritzsche. Prüfmethode zur Charakterisierung des Auftretens von LME beim Widerstandspunktschweißen von Stählen [Test methods to characterize the occurrence of LME during resistance spot welding of steels]. In: 24. DVS-Sondertagung Widerstandsschweißen. Proceedings; May 22-23; Duisburg; 2019; p. 171–183.

[18] Wintjes E, DiGiovanni C, He L, et al. Effect of Multiple Pulse Resistance Spot Welding Schedules on Liquid Metal Embrittlement Severity. *Journal of Manufacturing Science and Engineering*. 2019;141. DOI: 10.1115/1.4044099.

[19] Choi D-Y, Sharma A, Uhm S-H, et al. Liquid Metal Embrittlement of Resistance Spot Welded 1180 TRIP Steel: Effect of Electrode Force on Cracking Behavior. *Met. Mater. Int.* 2019;25:219–228.

[20] Frei J, Biegler M, Rethmeier M, et al. Investigation of liquid metal embrittlement of dual phase steel joints by electro-thermomechanical spot-welding simulation. *Science and Technology of Welding and Joining*. 2019;24:624–633.

[21] Böhne C, Meschut G, Biegler M, et al. Prevention of liquid metal embrittlement cracks in resistance spot welds by adaption of electrode geometry. *Science and Technology of Welding and Joining*. 2019;39:1–8.

[22] ISO 5821:2009 Resistance welding - Spot welding electrode caps (German

version). 2009. Germany: Deutsches Institut für Normung (DIN).

[23] SEP 1220-2:2011 Testing and Documentation Guideline for the Joinability of thin sheet of steel - Part 2: Resistance Spot Welding. 2011. Düsseldorf: Verlag Stahleisen GmbH.

[24] ISO/TS 18166:2016 Numerical welding simulation - execution and documentation (German version). 2016. Germany: Deutsches Institut für Normung (DIN).

[25] Coline B. Mechanical behaviour of a new automotive high manganese TWIP steel in the presence of liquid zinc [Dissertation]. Lyon; 2011.

[26] Marder AR. The metallurgy of zinc-coated steel. Progress in Materials Science. 2000:191–271.